Nanochitosan from Manufacture Shells of Mud Crab (*Scylla* sp.) and Its Application as Acne Patch

Novi Luthfiyana[1], Putri Wening Ratrinia[2], Nusaibah[3], and Mutia Khoirun Nisa[4]

OPEN ACCESS

[1] Department of Fisheries Product Technology, Universitas Borneo Tarakan. Jl. Amal Lama, Tarakan 77115, North Kalimantan, Indonesia.

[2] Department of Marine Processing Product, Politeknik Kelautan dan Perikanan Dumai, Jl Wan Amir No 1, Dumai, 28824, Riau, Indonesia

[3] Department of Marine Processing Product, Politeknik Kelautan dan Perikanan Pangandaran. Jl. Raya Babakan Km 2, Babakan, Pangandaran 46396, West Java, Indonesia

[4] Faculty of Biology, Universitas Gadjah Mada. Jl.Teknika Selatan, Sendowo, Sinduadi, Mlati, Sleman, special Region of Yogyakarta 55281, Indonesia

*Corresponding Author: luthfiyananovi@borneo.ac.id

Received: 2 March 2024

Accepted: 31 July 2024

Published: 31 August 2024

Academic Editor: Ima Wijayanti, Ph.D.

 Accreditation Number:148/M/KPT/2020. ISSN: 2089-5690, e-ISSN: 2406-9272. https://doi.org/10.15578/squalen.928

Abstract

Chitosan is a potential raw material for marine cosmetics with antibacterial, anti-inflammatory properties and can stimulate collagen synthesis in the skin. This research aimed to obtain nano-sized chitosan (nanochitosan) from mud crab (*Scylla* sp.) shells and apply it as a cosmetic acne patch. The parameters used to characterize nanochitosan are particle size, polydispersity index, zeta potential and morphology. Meanwhile, the parameters of the Acne patch produced are characterized by physical appearance and ance bacterial activity. The results revealed that nanochitosan had an average size of 35.20 ±1.66 nm, the highest intensity of 11.70±1.25, polydispersity of 0.274±0.10, and zeta potential of 42.9±1.41 mV. The morphology of nanochitosan is in the form of broken rods, not hollow and irregular but uniform. Its elements include carbon, oxygen, magnesium, aluminum, phosphorus, and calcium. The acne patches resulting from the addition of 0 mg (K0), 50 mg (K1), 100 mg (K2), and 150 mg (K3) were opaque white, slightly transparent, smooth, elastic, and odorless. The thickness varies, namely, 0.014 ± 0.002 mm (K0), 0.017 ± 0.002 mm (K1), 0.022 ± 0.004 mm (K2), and 0.031 ± 0.005 mm (K3). The weight variations were 0.019 ± 0.001 mg (K0), 0.026 ± 0.005 mg (K1), 0.033 ± 0.002 mg (K2), and 0.047 ± 0.013 mg (K3). The moisture loss varied, namely, 7.525 ± 0.054% (K0), 3.201 ± 0.487% (K1), 2.741 ± 0.279% (K2), and 2.017 ± 0.290% (K3). Acne patches K1, K2, and K3 were proven to be able to inhibit the activity of acne bacteria *Propionibacterium acnes* (9.5 ± 0.25 mm, 10.67 ± 0.76 mm, and 9.17 ± 0.76 mm), *Staphylococcus epidermidis* (9.33 ± 1.15 mm, 13.67 ± 2.02 mm, and 8.67 ± 1.89 mm), and *S. aureus* (10.33 ± 0.25 mm, 11.83 ± 0.76 mm, and 8.66 ± 0.76 mm). This research succeeded in obtaining chitosan from crab shells (*Scylla* sp) in nano size and acne patches with the addition of nanochitosan effectively inhibited the growth of acne bacteria.

Keywords: bacterial acne, chitosan, nanoparticles, physicochemistry

Introduction

There has been progress in the cosmetics industry despite the health crisis occurring in all countries caused by the COVID-19 pandemic. According to the Research and Market 2020–2027 Global Cosmetic Skin Care Industry report, the valuation value of world cosmetic sales in 2020 reached USD 145.3 billion and estimated to continue to grow by 3.6% per year from 2020 to 2027 (Amberg & Fogarassy, 2019). Marine resources are renowned for their content of biologically active substances and their excellent potential for application in the cosmetics industry. Kulka-Kamińska et al. (2020) reported that chitosan biopolymer is not included in the list of substances prohibited in cosmetics by the FDA. It is beneficial in cosmetic formulations because it can bind water and hydrate the skin as a thickener, rheology modifier, and emulsion stabilizer. Aflakseir et al. (2021tions, namely, protection, absorption, temperature regulation, defense, storage, and synthesis (Casadidio et al. 2020). Chitosan application to the skin surface can help in heal wound tissue by forming tissue structure, stimulating collagen synthesis, and maintaining good air permeability. Chitosan possesses good biocompatibility and biodegradability properties; antibacterial, hemostatic, and anti-inflammatory properties; good absorption of exudate; and enhanced tissue regeneration and growth of skin collagen fibers (Peng et al. 2022). The seafood processing industry produces around 6–8 million tons of shell waste. The use of chitosan has the potential to bring ecological and economic benefits because it

produces biopolymers from renewable resources (Chakravarty & Edwards 2022). Thus, to improve the effectiveness of chitosan, it was modified to nano size.

Chitosan being changed into nano size will enhance its stability and biological properties as an active substance in cosmetic preparations. Nano-sized chitosan can improve the absorption of macromolecular compounds, reduce irritating effects, and penetrate the spaces between cells and is flexible to be combined with various technologies (Rizeq et al. 2019). Chitosan nanoparticles can incorporate natural or chemical compounds as antimicrobial agents that show higher antimicrobial activity than chitosan (Ramezani et al. 2015). Nanochitosan is utilized for skin care because this compound can be formulated as a gel, fiber, or porous matrix that can be used to hydrate the skin and as an anti-aging or anti-acne cosmetic therapy (Ferreira et al. 2022). Chitosan-alginate nanoparticles are very promising for the treatment of acne disease because they show antimicrobial and anti-inflammatory properties (Friedman et al. 2013), chitosan-coated silver nanoparticles have also been shown to burn healing (Oryan et al. 2018), and antifungal (Bonilla et al. 2021). Based on chitosan's properties and advantages that have been explained, changing chitosan particles into nano size is very effective as a raw material for cosmetics because it is more targeted with minimal side effects. An acne patch is one type of cosmetic product that has the potential to accommodate the properties of nano-sized chitosan (nanochitosan) and is currently in great demand.

Acne patches absorb the fluid contained in acne while covering and protecting acne from dirt, dust, and bacteria that can stick to it. This way, the risk of worsening the existing acne brought by these contaminants can be minimized (Kuo et al. 2021). Since this skin care product is believed to get rid of acne in a swift manner, acne patches have become increasingly popular (Qothrunnadaa & Hasanah, 2021). Several studies revealed chitosan's ability to form films, inhibit the growth of acne-causing bacteria, and contain antioxidants. Vivcharenko et al. (2020) reported that chitosan-based films have good permeability, large surface area, and unique antibacterial properties. Zhang et al. (2020) reported that due to the antibacterial properties of chitosan when formulated as a hydrogel, film, or wound dressing sponge, it can be a good wound care material for infection prevention and treatment. Ma et al. (2017) revealed that chitosan films that contain glycerin as a strengthening agent can be utilized as wound dressings, inhibiting infections caused by bacteria. Luthfiyana et al. (2022) reported that a 1% concentration of chitosan from mud crab shells could inhibit the activity of *Staphylococcus aureus* bacteria by 13.5 mm, *S. epidermidis* by 12.5 mm, and *Propionibacterium acnes* by 34.5 mm. This indicates that chitosan can be an antibacterial solution to acne problems. This research aimed to obtain chitosan from nano-sized crab shells (*Scylla* sp.) and practically apply it in the form of acne patches. Previous research has explained that mud crab shell chitosan can inhibit the growth of bacteria that cause acne. Hence, changing the particle into nano size and formulating it into an acne patch is expected to be more effective.

Material and Methods

Mud crab (*Scylla* sp.) shell samples as raw material for nanochitosan were obtained from soft-shell crab cultivation in Tarakan, North Kalimantan, Indonesia. Research and analysis materials consisted of HCl (Bio-Rad, USA), NaOH (Bio-Rad, USA, filter paper (Whatman No 42), acetic acid (Merck, Germany), glycerol (Merck, Germany), HEC/hydroxyethyl cellulose (Merck, Germany), and HPMC/ hydroxypropyl methylcellulose (Merck, Germany), Pectin (Merck, Germany), Tween (Merck, Germany), PEG 400 (Bio-Rad, USA). The equipment for this research used includes an oven (Memmerh), analytical balance (AND GF-100), desiccator (DURAN Valumfest), blender (Panasonic MX-E310WSR), scanning electron microscopy energy dispersive X-ray spectroscopy (QUANTA 650), fourier transform infraRed (Shimadzu, IRSpirit- T), hot plate and stirrer (IKA C-MAG HS 4), and various glassware (Pyrex).

Preparation of Nanochitosan

Making nanochitosan from mud crab shells begins with sample preparation, producing chitosan, and then modifying the chitosan into a nano size referring to Luthfiyana et al. (2022). This method was chosen because it produces chitosan with a deacetylation degree of 76%, which is by SNI standards, so the ability of chitosan as an active substance is optimal. Sample preparation was performed by cleaning, drying, and grinding the mud crab shells into a 50-mesh powder. Producing chitosan comprises three stages. The first stage is deproteination, carried out by soaking 200 g of mud crab shell powder in a 3N NaOH solution (1:10 w/v) at 80°C for 60 min. The second stage is demineralization by soaking mud crab shell powder in 1N HCl solution (1:15 w/v) at room temperature for 120 min. The third stage is deacetylation by soaking mud crab shell powder in 60% NaOH solution (1:10 w/v) at 140°C for 60 min. At each stage, neutralization was conducted using distilled water to pH 7 and drying via an oven at a temperature of 65°C. Chitosan size modification was conducted by dissolving 0.2 g of chitosan in 100 mL of 1% acetic acid solution. The chitosan solution was then stirred using a magnetic

stirrer for 8 h at a speed of 3,000 rpm. The chitosan solution was then added to 50 µL of Tween 80 (0.1%) and stirred for 2 h. The next stage was slowly adding 7 mL of 0.1% sodium tripolyphosphate (Na TPP) and stirring for 2 h. The nanochitosan solution is then converted into powder form via freeze-drying. The nanochitosan powder is then stored in a tight glass container before use.

Preparation of Acne Patch

Acne patch formulation refers to manufacturing the hydrogel patch Qothrunnadaa and Hasanah (2021) with modifications. Table 1 presents the ingredients and concentrations utilized in the acne patch formula. The first stage, preparation 1, was carried out by dissolving pectin, HEC (hydroxyethyl cellulose), and HPMC (hydroxypropyl methylcellulose) using distilled water at a temperature of 80°C. In the second stage, preparation 2, nanochitosan made with mud crab shell was dissolved in 1% acetic acid at a temperature of 80°C until it was homogeneous and formed a clear gel. The third stage, preparation 3, was made by mixing preparation 1, preparation 2, glycerol, Tween 80, and PEG 400. Each stage was stirred using a magnetic stirrer at 1,500 rpm. The solution (preparation 3) was left to stand first to remove bubbles and was then poured into glass Petri dishes (150x25 mm) and dried at 60°C for 48 h.

Table 1. Acne patch formula

Ingredients	Formula (mg)			
	KO	K1	K2	K3
Nanochitosan Mud crab shells	0	50	100	150
HPMC	350	350	350	350
HEC	2,800	2,800	2,800	2,800
Pectin	700	700	700	700
Acetic acid	20	20	20	20
distilled water	200	200	200	200
Glycerol	2	2	2	2
Tween 80	2	2	2	2
PEG 400	120	120	120	120

Characterization of Nanochitosan (*Scylla* sp.)

Particle Size, Polydispersity Index, and Zeta Potential Analysis

Determination of diameter, particle distribution, and zeta potential (ZP) was conducted using the particle size analyzer tool via the DLS/dynamic light scattering method referring to Honary and Zahir (2013). A Zeta Sizer Nano (ZS-90, Malvern, UK) evaluated particle size, polydispersity index (PDI), and ZP. Two drops of the nanochitosan solution were pipetted, and then, 5 mL of distilled water was added. Then, 3 mL of nanochitosan solution was put into the cell/cuvette, ensuring that there were no air bubbles. Visible light is shot into the cuvette, causing diffraction to occur. Particle size measurement employs the principle of visible light scattering. Particle diameter, PDI, and ZP measurements were carried out using scattering angles of 90° and 173°. The measurement results are displayed on the monitor screen.

Scanning Electron Microscopy and Energy-Dispersive X-ray spectroscopy

Scanning Electron Microscopy and Energy-Dispersive X-ray spectroscopy (SEM-EDS, Quanta 650,USA) analysis followed the procedure described by Girão et al. (2017). The carbon tex attached to the sample was cut into a rectangular shape with a size of ±1 cm. The sample attached to the carbon tex paper was stored on a stub and was then blown and placed in the chamber. This test was carried out with a low vacuum because the sample was a nonconductor. The analyzed sample could be viewed on the monitor screen at a particular magnification.

Physicochemical Characterization of Acne Patch (*Scylla* sp.)

Physical Appearance

A physical appearance examination was conducted by observing the color, texture, and odor of the nanochitosan acne patch produced and then describing the appearance of the patch. Visual observation of the resulting acne patches involved 15 respondents, with the criteria for using three commercial acne patch products. (Qothrunnadaa & Hasanah, 2021).

Thickness

The thickness of the acne patch was measured using a caliper with an accuracy of 0.01 mm. Measurements were performed at three different points, and three patches were selected for each formulation. Acne patch thickness is determined by calculating the average value of each formula (Pathel et al. 2012).

Weight Variation

Three samples were randomly taken from each acne patch formula, and the weight was weighed. The weight variation value for each acne patch formula is calculated from the average weight (Usman et al. 2023).

Moisture Loss

Moisture loss values were calculated based on the procedure by Usman et al. (2023). Acne patches were weighed and stored in a saturated potassium chloride solution desiccator for 3 days. The patch is weighed again, and the percentage of moisture content is determined using the following formula:

Acne Bacterial Activity of Acne Patch

The antibacterial activity of acne patches is tested by rejuvenating and preparing a bacterial liquid culture first. The types of bacteria used were *P. acnes* ATCC 11827, *S. epidermidis* FNCC 0048, and *S. aureus* FNCC 0047 taken from the Center for Food and Nutrition Studies (P SPG) Gadjah Mada University, Yogyakarta, Indonesia. *P. acnes* bacteria were rejuvenated based on the research method of Vaz et al. (2018). The acne patch activity test involved dissolving 3.8 g of Mueller Hinton agar (MHA) in 100 mL of distilled water, sterilizing it in an autoclave at 121°C for 15 min, and pouring it into Petri dishes to cool. Bacterial liquid cultures of *P. acnes*, *S. epidermidis*, and *S. aureus* were added to the still-liquid MHA medium, and nanochitosan acne patches with varying concentrations (K0: 0 mg, K1: 50 mg, K2: 100 mg, and K3: 150 mg) were placed into the MHA treated with bacteria. The dishes were then incubated at 35°C for 24 h, and the inhibitory power of chitosan against

$$\%\ Moisture\ loss = \frac{(\text{Initial wt} - \text{Final wt})}{\text{Final wt}} \times 100\%$$

P. acnes bacteria was determined by measuring the clear zone formed. The results of this study were then compared with commercial acne patch products.

Data Analysis

The analysis of the characteristics of mud crab shell nanochitosan was presented descriptively. The antibacterial activity of the acne patch preparation was analyzed using a one-factor analysis of variance (ANOVA) test with the addition of mud crab shell nanochitosan at 0, 50, 100, and 150 mg. Each experiment was conducted thrice. Data were analyzed using ANOVA at 95% confidence intervals. If there was a significant difference, a further test was carried out using the least significant difference test.

Results and Discussion

Characterization Nanochitosan of (*Scylla* sp.)—Mean Particle Size, Polydispersity, and Zeta Potential

Mud crab shell (*Scylla* sp.) chitosan nanoparticles made using the ionic gelation method had the highest intensity of 11.70±1.25 nm with a mean particle size value of 35.20±1.66 nm (Figure 1). The results of this research confirm that the chitosan obtained is nano-sized. Jhaveri et al. (2021) stated that nanoparticles have sizes ranging from 1 to 100 nm. Sreekumar et al. (2018) reported that adding Na TPP affects the size of the chitosan particles produced because of its characteristic as a cross-linking agent and its ability to strengthen the chitosan nanoparticle matrix to be more stable.

The PDI produced in mud crab shell nanochitosan was 0.274±0.10. The PDI value is an indicator of overall nanoparticle uniformity. Clayton et al. (2016) reported that higher PDI values indicate larger or aggregated particles. Lower PDI corresponds to smaller-sized monodisperse particles and no aggregation. Wu et al. (2017) stated that the PDI is used to analyze the homogeneity of particle size diameter distribution. Heterogeneous dispersed particle size can increase the occurrence of agglomeration.

The ZP determines the quality of the resulting nanoparticles. The ZP of mud crab shell nanochitosan is 42.9 ±1.41mV (Figure 1). The ZP value determines the nature of the resulting charge. The nature of the particle charge will later influence the stability of the particle. Luthfiyana et al. (2022) reported that ZP is a parameter of the electric charge between colloidal particles. The greater the ZP value, the more it inhibits flocculation.

The ZP is more than 30 mV and has a positive charge. A negative or positive charge indicates that there is a greater repulsive force, making it able to prevent aggregation and provide good stability. Jain et al. (2014) revealed that the positive ZP charge is due to the influence of the amount of chitosan being more notable than the amount of sodium alginate, causing many amine groups in the chitosan to not bind to the sodium alginate. Conversely, the negative ZP value is due to the amount of chitosan that is less than that of sodium alginate; hence, there are still free carboxyl groups in the sodium alginate. Shetta et al. (2019) stated that a higher surface charge could cause a solid electrostatic repulsion force on nanoparticles, thereby preventing aggregation. A ZP value of >±30 mV indicates that nanochitosan has high stability, a ZP of around ±20 mV indicates medium- or short-term stability, and a ZP value of around ±5 mV will result in low stability and aggregation will quickly occur. Rodriguez et al. (2013) stated that the surfactant is

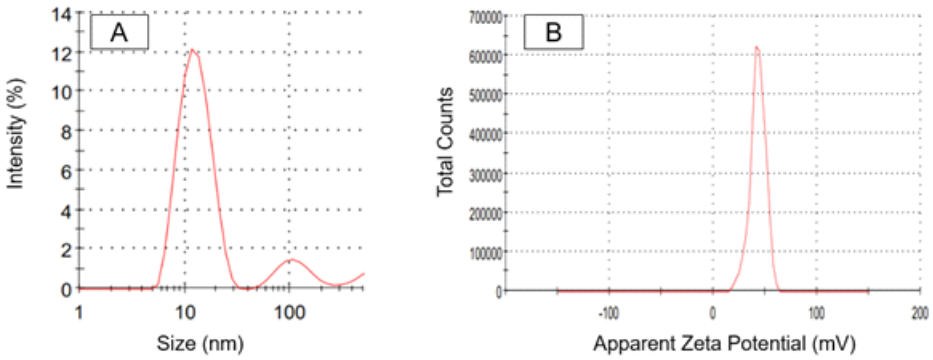

Figure 1. Size distribution intensity (A) and zeta potential (B) of nanochitosan from mud crab shells *Scylla* sp.

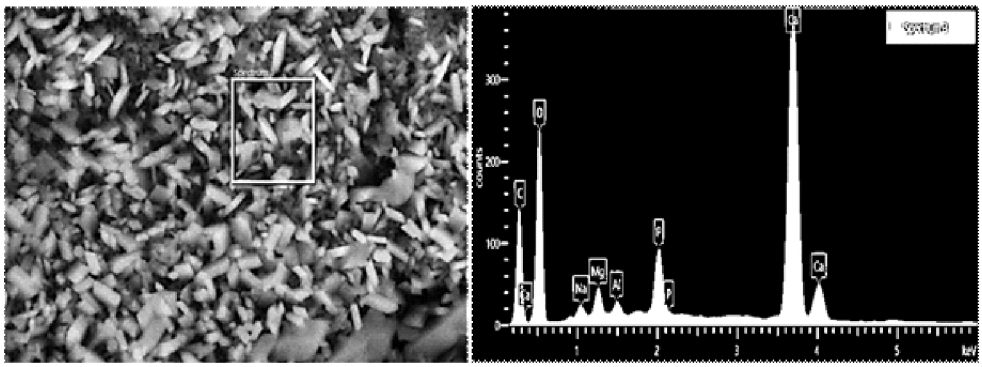

(A) (B)

Figure 2. Morphology of nanochitosan from mud crab shells (*Scylla* sp) (A) and element content based on energy-dispersive X-ray spectrum (B) with 1,000 times magnification.

employed to reduce the tension between the solid–liquid surface so that a repulsive force is generated between the particles, which prevents aggregation and maintains stability.

SEM-EDS

The morphology and element content of mud crab (*Scylla* sp.) shell nanochitosan were identified using SEM-EDS (Kweinor et al. 2021; Sultan, 2022). The surface morphology of nanochitosan seen using SEM with a magnification of 1000 times shows rod-shaped fractures, not hollow and irregular but mostly uniform (Figure 2A). The EDS results show that the element content in nanochitosan comprises carbon, oxygen, magnesium, aluminum, phosphorus, and calcium (Figure 2B). Lima et al. (2014) reported that the morphology of pure chitosan membranes observed using SEM had a porous surface and was characterized as a solid membrane. The shape of chitosan changes due to chemical activity and the formation of agglomerates. Micrographs of chitosan membranes with Na TPP showing rod-shaped morphology with different sizes distributed throughout the membrane surface can be verified.

Chitosan contains several elements, namely, carbon, oxygen, magnesium, aluminum, phosphorus, and calcium (Figure 2B). Visible carbon and oxygen are the constituents of chitosan, whereas magnesium, aluminum, phosphorus, and calcium are elements contained in mud crab shells. Luthfiyana et al. (2022) reported that other elements were visible in chitosan due to a less-than-optimal demineralization process. Dong et al. (2013) reported the EDS spectrum of the chitosan membrane itself, showing the elements O, C, and N in the chitosan membrane itself. The EDS spectrum of nanochitosan changes its chemical composition. Other elements are also visible in nanochitosan, possibly due to cross-linking between the chitosan chains and Na TPP.

Physicochemical Characteristics of Acne Patch (*Scylla* sp.)

Nanochitosan as an acne patch preparation can increase users' comfort, safety, cover acne infections and prevent contamination (Suryani et al., 2019). Physicochemical evaluation of acne patches added with nanochitosan from mud crab shells (*Scylla* sp.) was analyzed using the parameters of physical appearance,

thickness, weight variation, and moisture content. Table 2 presents the physicochemical results of the acne patch preparation.

The physical appearance results show that the four acne patch formulas with the addition of nanochitosan from mud crab shells are opaque white and slightly transparent, and the surface texture is smooth, thin, elastic, and odorless (Table 2). Rizki et al. (2020) reported that a good patch has a physical form that is flexible, thin, homogeneous, smooth, and does not produce a disturbing aroma. A good patch has an elastic texture that does not become brittle or tear. Qothrunnadaa and Hasanh (2021) reported that the patch has a good film consistency, making it tear- or breakage-resistant during storage. The elasticity of the patch is affected by the combination of hydrophilic and hydrophobic polymers. The combination of pectin, HEC, and HPMC (hydrophilic) and a mixture of PEG 400 and glycerol, which is hydrophobic, can increase the elasticity and strength of the acne patch preparation so that it does not break and crumble easily.

The thickness of the acne patch produced varies for each formula, ranging from 0.014 ± 0.002 mm to 0.031 ± 0.005 mm (Table 2). The higher the concentration of nanochitosan added, the thicker the resulting acne patch formula solution will be. Patel et al. (2018) reported that the greater the concentration of the penetration enhancer, the greater the thickness of the resulting acne patch. The viscosity of a solution will affect the distribution of the solution in the mold. The thicker the solution, the lower its spreading power, resulting in a higher patch thickness. Pandey et al. (2014) stated that thickness can affect the release of active substances from the preparation. If the acne patch is thick, releasing the active substance will take longer to diffuse from the membrane. Thin acne patch preparations will be easier and more comfortable to use. The difference in patch thickness results can also be influenced by the technique of pouring the patch into the mold. Singh and Bali (2016) reported that the thickness of the formulated transdermal patch meets the requirements for transdermal patch thickness if it is 1 mm.

The greater the concentration of nanochitosan added, the greater the weight of the patch produced (Table 2). The average value and standard deviation obtained show that all formulas meet the requirements with a coefficient of variance value of 5%. Pastore et al. (2015) stated that the weight uniformity test aims to determine the uniformity of the weight of the resulting patches. Weight uniformity can also indicate the uniformity of the active substance content in the patch and ensure that each patch contains several active ingredients in the correct and even dosage.

Moisture loss is a parameter employed to determine the patch's ability to absorb moisture. Table 2 shows that moisture loss without adding chitosan (hydrophobic) has the highest value of 7.525 ± 0.054%. A low absorption percentage indicates a relatively stable patch that tends to be protected from microorganisms. Moisture absorption increases as the hydrophilicity of the polymer or plasticizer used increases. A good patch should not be too damp because it will easily break or tear and should not be too dry because it will break easily or become brittle. Byeon et al. (2017) stated that using hydrophobic polymers could affect the moisture loss of the preparation; the higher the concentration of hydrophilic polymer used, the greater the percentage of moisture loss. According to Suryani et al. (2019), there are no set standards for how much water should be in patch preparations. The lower amount of water content in the patch can cause the preparation to become brittle. Conversely, higher water content can increase the risk of microbial contamination.

Acne Bacterial Activity of Acne Patches

Acne patches with nanochitosan K1, K2, and K3 showed antibacterial activity by forming a clear zone. By contrast, K0 and KM did not show antibacterial activity against *P. acnes*, *S. epidermidis*, and *S. aureus* (Figure 3). The highest zone of inhibition from the

Table 2. Physicochemical of acne patches

Parameter	*Formula			
	K0	K1	K2	K3
Physical appearance				
Color	opaque white slightly transparent	opaque white slightly transparent	opaque white slightly transparent	opaque white slightly transparent
Texture	smooth, thin, and elastic	smooth, thin, and elastic	smooth, thin, and elastic	smooth, thin, and elastic
Odor	odorless	odorless	odorless	odorless
Thickness (mm)	0.014 ± 0.002	0.017 ± 0.002	0.022 ± 0.004	0.031 ± 0.005
Weight variation (mg)	0.019 ± 0.001	0.026 ± 0.005	0.033 ± 0.002	0.047 ± 0.013
Moisture loss (%)	7.525 ± 0.054	3.201 ± 0.487	2.741 ± 0.279	2.017 ± 0.290

*Acne patch formula with the addition of nanochitosan from mud crab shells K0: 0 mg, K1: 50 mg, K2: 100 mg, and K3: 150 mg.

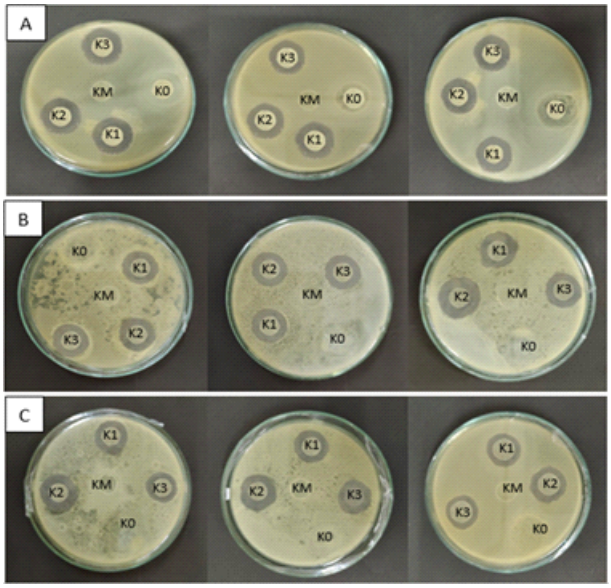

Figure 3. Inhibition zone of the acne patch preparation with the addition of mud crab shell nanochitosan K0: 0 mg, K1: 50 mg, K2: 100 mg, K3: 150 mg, and KM: commercial against *P. acnes* (A), *S. epidermidis* (B), and *S. aureus*(C).

Table 3. Acne patch inhibition zone against acne bacteria

Acne Bacteria	*Acne Patch Inhibition Zone				
	KM	K0	K1	K2	K3
P. acnes ATCC 11827	0 ± 0	0 ± 0	9.5^{b} ± 0.25	10.67^{a} ± 0.76	9.17^{b} ± 0.76
S. epidermidis FNCC 0048	0 ± 0	0 ± 0	9.33^{b} ± 1.15	13.67^{a} ± 2.02	8.67^{c} ± 1.89
*S. aureus*FNCC 0047	0 ± 0	0 ± 0	10.33^{b} ± 0.25	11.83^{a} ± 0.76	8.66^{c} ± 0.76

*Acne patch inhibition zone with the addition of nanochitosan from mud crab shells K0: 0 mg, K1: 50 mg, K2: 100 mg; K3: 150 mg, and KM: commercial acne patch. Letters from the same alphabet indicate non-significant at $p < 0.05$. The data were expressed as mean ± standard deviation of three replications.

results of the one-way ANOVA test and the LSD further test showed that the different concentrations of nanochitosan affected the antibacterial activity of the acne patch (Table 3).

The differences in antibacterial activity in the three treatments are likely due to several factors. Chandrasekaran et al. (2020) reported that several factors could influence the antimicrobial activity of nanochitosan, namely, the species of bacteria, bacterial growth curve, pH, concentration, ZP, molecular weight, and degree of acetylation. Additionally, nanochitosan has polycations with a broader surface charge density than chitosan when fighting bacteria. This causes the walls and membranes of the bacterial cells to be disrupted, and then, there is a leak of intracellular molecules, causing the bacterial cells to die. Furthermore, Duan et al. (2019) revealed that the mechanism of chitosan in inhibiting gram-positive bacteria is by binding to the plasma membrane and then inactivating enzymes and proteins, damaging DNA, and disrupting cell function and metabolic processes, which will ultimately cause cell death. Previous research stated that nanochitosan can be utilized to treat skin and has been proven to heal wounds (Zmejkoski et al. 2021). Sungkharak et al. (2016) reported that nanochitosan inhibits *P. acne* and *S. epidermis* bacteria more than chitosan, but both still have antibacterial activity. This statement was reinforced by Luthfiyana et al. (2022), who explained that chitosan can inhibit the acne-causing bacteria *P. acnes*, *S. epidermidis*, and *S. aureus* and is more effective in producing a higher clear zone if it is in its nano-sized form. Qothrunnadaa and Hasanah (2021) revealed that nanochitosan is a hydrophobic antibacterial agent that quickly diffuses through the lipid skin layer. The in vitro antibacterial test results show that the patch can be effective not only on the skin underneath but also on the surrounding skin. Based on the results, acne patches with nanochitosan are much more effective than commercial products in fighting the acne bacteria *P. acnes*, *S. epidermidis*, and *S. aureus*.

Acne patch K2 showed the best results in inhibiting *P. acnes, S. epidermidis,* and *S. aureus* bacteria (Table 4). This result is because the level of K3 viscosity influences the diffusion process. The antimicrobial activity of nanochitosan is realized by different mechanisms depending on the molecular weight of chitosan and its concentration. Too high a concentration will cause aggregates and inhibit diffusion (Kovács et al. 2023). The higher chitosan concentration makes the solution mixture too thick and concentrated, thereby reducing the diffusion ability of the patch into the bacterial growth medium and reducing the patch's inhibitory power against microbial growth (Syaefudin et al. 2023). The inhibition zone in a medium can be influenced by temperature and incubation time, suspension density, type of bacteria, and sample concentration used (Divya et al. 2017).

Conclusion

This research was successful in obtaining chitosan from crab shells (*Scylla* sp) with an average nano size of 35.20 nm and highest intensity of 11.70; the resulting PDI was 0.274 with a positively charged ZP of 42.9 mV. The morphology of nanochitosan from mud crab shells was successfully applied to acne patches, resulting in the best formula with the addition of 100 mg (K2) nanochitosan with physicochemical characteristics, that is, opaque white, slightly transparent, smooth, elastic, and odorless; a thickness of 0.022 ± 0.004 mm; a weight variation of 0.033 ± 0.002 mg; and moisture loss 2.741 ± 0.279%. The acne patch was proven to be able to inhibit the activity of the acne bacteria *P. acnes* (10.67a ± 0.76 mm), *S. epidermidis* (13.67a ± 2.02 mm), and *S. aureus* (11.83a ± 0.76 mm). Acne patches with the addition of nanochitosan are much more effective than commercial products.

Acknowledgments

The authors thank the Department of Fisheries Product Technology, Universitas Borneo Tarakan for fully facilitating this research. This study was funded by KEMENDIKBUD-RISTEK based on decree Contract number 008/UN51.9/ SP2H-LT/2023 through the scheme "Penelitian Dosen pemula (PDP)" 2023.

Supplementary Materials

Supplementary materials is not available for this article

References

Aûakseir, A., Jamali, S., Mollazadeh, J. (2021). Prevalence of Body Dysmorphic Disorder Among a Group of College Students in Shiraz. *Zahedan Journal of Research in Medical Sciences*, 23(2),e95247. https://doi.org/10.5812/zjrms.95247

Amberg, N., & Fogarassy, C. (2019). Green consumer behavior in the cosmetics market. *Resources*, 8(3), 137. https://doi.org/10.3390/resources8030137

Aranaz, I., Acosta, N., Civera, C., Elorza, B., Mingo, J., Castro, C., Gandía, M.D.l.L., & Heras, C.A. (2018). Cosmetics and cosmeceutical applications of chitin, chitosan and their derivatives. *Polymers*, 10(2), 213. https://doi.org/10.3390/polym10020213

Arancibia, M.Y., Alemán, A., Calvo, M.M., López-Caballero, M.E., Montero, P., & Gómez-Guillén, M.C. (2014). Antimicrobial and antioxidant chitosan solution senriched with active shrimp (*Litopenaeus vannamei*) waste materials. *Food Hydrocoll*, 35, 710-717. https://doi.org/10.1016/j.foodhyd.2013.08.026

Bonilla, J.J.A., Honorato, L., de Oliveira, D.F.C., Gonçalves, R.A., Guimarães, A., Miranda, K., Nimrichter, L. (2021). Silver chitosan nanocomposites as a potential treatment for superficial candidiasis. *Medical Mycology.* 59:993–1005. https://doi.10.1093/mmy/myab028

Byeon, S.Y., Cho, M.K., Shim, K.H., Kim, H.J., Song, H.G., & Shin, H.S. (2017). Development of a spirulina extract/alginate-imbedded pcl nanofibrous cosmetic patch. *Journal of Microbiology and Biotechnology*, 27(9),1657-1663. https://doi.org/10.4014/jmb.1701.01025

Casadidio, C., Butini, M.E., Trampuz, A., Di Luca, M., Censi, R., & Di Martino, P. (2018). Daptomycin-loaded biodegradable thermosensitive hydrogels enhance drug stability and foster bactericidal activity against *Staphylococcus aureus*.(2018). *European Journal of Pharmaceutics and Biopharmaceutics*, 130, 260–271. https://doi.org/10.1016/j.ejpb.2018.07.001

Chakravarty, J., & Edwards, T.A. (2022). Innovation from waste with biomass-derived chitin and chitosan as green and sustainable polymer: A review. *Energy Nexus*, 8(12),100149 https://doi.org/10.1016/j.nexus.2022.100149

Chandrasekaran, M., Kim, K.D., & Chun, S.C. (2020). Antibacterial activity of chitosan nanoparticles: a review. *Processes*. 8(9),1173. https://doi.org/10.3390/pr8091173

Christensen, G.J., Scholz, C.F., Enghild, J., Rohde, H., Kilian, M., Thürmer, A., Brzuszkiewicz, E., Lomholt, H.B., & Brüggemann, H. (2016). Antagonism between Staphylococcus epidermidis and Propionibacterium acnes and its genomic basis. *BMC Genomics*, 17, 152. https://doi.org/10.1186/s12864-016-2489-5

Clayton, K.N., Salameh, J.W., Wereley, S.T., & Kinzer-Ursem, T.L. (2016). Physical characterization of nanoparticle size and surface modification using particle scattering diffusometry. *Biomicrofluidics*. 10(5), 054107. https://doi.org/10.1063/1.4962992

Divya, K., Vijayan, S., George, T.K. & Jisha, M.S. (2017). Antimicrobial properties of chitosan nanoparticles: Mode of action and factors affecting activity. *Fibers and Polymers*, 18, 221–23. https://doi.org/10.1007/s12221-017-6690-1

Dong, Y., Ng, W.K., Shen, S., Kim, S., & Tan, R.B. (2013). Scalable ionic gelation synthesis of chitosan nanoparticles for drug delivery in static mixers. *Carbohydrate Polymers*.

94(2), 940-945. https://doi.org/10.1016/j.carbpol.2013.02.013

Duan, C., Xin, M., Jingru, K, Md. Iqbal, D., Lei, K., Avik, A., Xingye, Z., Junhua, Huq., Tanzina, N., & Yonghao. (2020). Chitosan as a preservative for fruits and vegetables: a review on chemistry and antimicrobial properties. *Journal of Bioresources and Bioproducts*, 4, 11-21. https://doi.org/10.21967/jbb.v4i1.189

Ferreira, P.G., Ferreira, V.F., da Silva, F.C., Freitas, C.S., Pereira, P.R., Paschoalin, V.M.F. (2022). Chitosans and Nanochitosans: Recent Advances in Skin Protection, Regeneration, and Repair. *Pharmaceutics*, 14(6),1307. https://doi.10.3390/pharmaceutics14061307

Friedman, A., Phan, J., Schairer, D.O., Champer, J., Qin, M., Pirouz A., Blecher-Paz, K., Oren, A., Liu, P.T., Modlin, R. (2013). Antimicrobial and Anti-Inflammatory Activity of Chitosan–Alginate Nanoparticles: A Targeted Therapy for Cutaneous Pathogens. *Journal of Investigative Dermatology*. 133:1231–1239. https://doi.org/10.1038/jid.2012.399

Girão, A.V., Caputo, G., & Ferro, M.C. (2017). Application of Scanning Electron Microscopy–Energy Dispersive X-Ray Spectroscopy (SEM-EDS), *Comprehensive Analytical Chemistry*, 75,153-168. https://doi.org/10.1016/bs.coac.2016.10.002

Honary, S. & Zahir, F. (2013). Effect of zeta potential on the properties of nano-drug delivery systems-A review (Part 1). *Tropical Journal of Pharmaceutical Research*, 12 (2), https://doi.org/10.4314/tjpr.v12i2.19

Jain, A.,Thakur, K., Kush, P., & Jain, U.K. (2014). Docetaxel loaded chitosan nanoparticles: Formulation, characterization and cytotoxicity studies. *International Journal of Biological Macromolecules*, 69, 546-553. https://doi.org/10.1016/j.ijbiomac.2014.06.029

Jhaveri, J., Raichura, Z., Khan, T., Momin, M., & Omri, A. (2021). Chitosan nanoparticles-insight into properties, functionalization and applications in drug delivery and theranostics. *Molecules*, 26(2), 272. https://doi.org/10.3390/molecules26020272

Kulka-Kamiñska, Karolina & Alina, S. (2023). Chitosan Based Materials in Cosmetic Applications: A Review. *Molecules*, 28(4), 1817. https://doi.org/10.3390/molecules28041817

Kuo, C.W., Chiu, Y.F., Wu, M.H., Li, M.H., Wu, C.N., Chen, W.S., & Huang, C.H. (2021). Gelatin/chitosan bilayer patches loaded with cortex *phellodendron amurense*/*centella asiatica* extracts for anti-acne application. *Polymers*, *13*, 579. https://doi.org/10.3390/polym13040579

Kim, S,H., Eom, S.H., Yu, D., Lee, M.S., & Kim, Y.M. (2017). Oligochitosan as a potential anti-acne vulgaris agent: combined antibacterial effects against *Propionibacterium acnes*. *Food Science and Biotechnology*, 26(4),1029-1036. https://doi.org/10.1007%2Fs10068-017-0118-y

Kovács, R., Erdélyi, L., Fenyvesi, F., Balla, N., Kovács, F., Vámosi, G., Klusóczki, Á., Gyöngyösi, A., Bácskay, I., Vecsernyés, M., & Váradi, J. (2022). Concentration-dependent antibacterial activity of chitosan on *Lactobacillus plantarum*. *Pharmaceutics*, 15(1), 18. https://doi.org/10.3390/pharmaceutics15010018

Kweinor Tetteh, E., Obotey Ezugbe, E., Asante-Sackey, D., Armah, E.K., & Rathilal, S. (2021). Response surface methodology: photocatalytic degradation kinetics of basic blue 41 dye using activated carbon with tio2. *Molecules*, 26(4), 1068. https://doi.org/10.3390/molecules26041068

Lima, H.A., Lia, F. M. V., & Ramdayal, S. (2014). Preparation and characterization of chitosan-insulin-tripolypho sphate membrane for controlled drug release: effect of cross linking agent. *Journal of Biomaterials and Nanobiotechnology*. 5(4), 211-219. http://dx.doi.org/10.4236/jbnb.2014.54025

Luthfiyana, N., Bija, S., Anwar, E., Laksmitawati, D.E., & Rosalinda, G.L. (2022). Characteristics and activity of chitosan from mud crab shells on acne bacteria: *Staphylococcus aureus*, *S. epidermidis* and *Propionibacterium acnes*. *Biodiversitas*, 23(12), 6645-6651. https://doi.org/10.13057/biodiv/d231263

Luthfiyana, N., Bija, S., Nugraeni, C.H., Lembang, M.S., Anwar, E. Laksmiwati, D.R., Nusaibah, Ratrinia, P.W., & Mukmainna. (2022). Characteristics and antibacterial activity of chitosan nanoparticlesfrom mangrove crab shell (*Scylla* sp.) in Tarakan Waters, North Kalimantan, Indonesia. *Biodiversitas*, 23 (8), 4018-4025. https://doi.org/10.13057/biodiv/d230820

Ma, Y., Xin, L., Tan, H., Fan, M., Li, J., Jia, Y., Ling, Z., Chen, Y., & Hu, X. (2017). Chitosan membrane dressings toughened by glycerol to load antibacterial drugs for wound healing. *Materials Science and Engineering*, 1(81), 522-531. https://doi.org/10.1016/j.msec.2017.08.052

Oryan, A., Alemzadeh, E., Tashkhourian, J., Ana, S.F.N. (2018). Topical delivery of chitosan-capped silver nanoparticles speeds up healing in burn wounds: A preclinical study. *Carbohydrate Polymers*. 200:82–92. https://doi.10.1016/j.carbpol.2018.07.077

Pandey, A., Mittal, A., Chauhan, N., & Alam, S. (2014). Role of surfactants as penetration enhancer in transdermal drug delivery system. *Journal of Molecular Pharmaceutics Organic Process Research*, 02(02), 113. http://dx.doi.org/10.4172/2329-9053.1000113

Pastore, M.N., Kalia, Y.N., Horstmann, M., & Roberts, M.S. (2015). Transdermal patches: history, development and pharmacology. *British Journal of Pharmacology*, 172(9), 2179-2209. https://doi.org/10.1111/bph.13059

Patel, R., Patel, A., Prajapati, B., Shinde, G., & Dharamsi, A. (2018). transdermal drug delivery systems: a mini review. *International Journal of Advanced Research*, 6(5), 891–900. http://dx.doi.org/10.21474/IJAR01/7109.

Peng, W., Li, D., Dai, K., Wang, Y., Song, P., Li, H., Tang, P., Zhang, Z., Li, Z., & Zhou, Y. (2022). Recent progress of collagen, chitosan, alginate and other hydrogels in skin repair and wound dressing applications. *International Journal of Biological Macromolecules, 298*, 400–408. https://doi.org/10.1016/j.ijbiomac.2022.03.002

Qothrunnadaa, T., & Hasanah, A. N. (2021). Patches for acne treatment: an update on the formulation and stability test. *International Journal of Applied Pharmaceutics*, 13(4), 21–26. https://doi.org/10.22159/ijap.2021.v13s4.43812

Ramezani, Z., Zarei, M., & Raminnejad, N. 2015. Comparing the effectiveness of chitosan and nanochitosan coatings on the quality of refrigerated silver carp fillets. *Food Control*. 51, 43-48. http://dx.doi.org/10.1016/j.foodcont.2014.11.015

Rizeq, B. R., Younes, N. N., Rasool, K., & Nasrallah, G. K. (2019). Synthesis, bioapplications, and toxicity evaluation of chitosan-based nanoparticles. *International Journal of*

Molecular Sciences, 20 (22), 5776. https://doi.org/10.3390/ijms20225776

Riski, R., Awaluddin, A., & Riko, A. (2020). Formulation and effectivity study of antipyretic patch from ethanol extract of bitter melon leaf (*Momordica charantia* L.). *Journal of Pharmaceutical and Biomedical Sciences*, 5(1):1–6. https://dx.doi.org/10.32814/jpms.v5i1.111

Rodriguez, V.A., Bolla, P.K., Kalhapure, R.S., Boddu, S.H.S., Neupane, R., Franco, J., & Renukuntla, J. (2019). Preparation and characterization of furosemide-silver complex loaded chitosan nanoparticles. *Processes, 7*(4), 206. https://doi.org/10.3390/pr7040206

Senthilkumar, P., Yaswant, G., Kavitha, S., Chandramohan, E., Kowsalya, G., Vijay, R., Sudhagar, B., & Kumar, D.S.R.S. (2019). Preparation and characterization of hybrid chitosan-silver nanoparticles (Chi-Ag NPs); a potential antibacterial agent. *International Journal of Biological Macromolecules*, 141, 290–298. https://doi.org/10.1016/j.ijbiomac.2019.08.234

Shetta, A., Kegere, J., & Mamdouh, W. (2019). Comparative study of encapsulated peppermint and green tea essential oils in chitosan nanoparticles: Encapsulation, thermal stability, in-vitro release, antioxidant and antibacterial activities. *International Journal of Biological Macromolecules. 126*, 731–742. https://doi.org/10.1016/j.ijbiomac.2018.12.161

Singh, A., & Bali, A. Formulation and characterization of transdermal patches for controlled delivery of duloxetine hydrochloride. *Journal Analytical Science Technology, 7, (25).* https://doi.org/10.1186/s40543-016-0105-6

Sreekumar, S., Goycoolea, F.M., Moerschbacher, B.M., Rivera-Rodriguez, G.R. (2018). Parameters influencing the size of chitosan-TPP nano- and microparticles. *Scientific Report*. 8(1), 4695. https://doi.org/10.1038/s41598-018-23064-4

Sultan M., Siddique M., Khan R., Fallatah A.M., Fatima N., Shahzadi, I., Waheed U., Bilal, M., Ali, A., & Abbasi, A.M. (2022). Ligustrum lucidum leaf extract-assisted green synthesis of silver nanoparticles and nanoadsorbents having potential in ultrasound-assisted adsorptive removal of methylene blue dye from wastewater and antimicrobial activity. *Materials*,15(5),1637. https://doi.org/10.3390/ma15051637

Sungkharak, S., Supasit, N., Choopan, S., & Ungphaiboon, S. (2016). Antibacterial activity against acne involved bacteria of chitosan in a soluble state and as nanoparticles. *Chiang Mai Journal of Science*. *43*(5), 1150–1159. http://cmuir.cmu.ac.th/jspui/handle/6653943832/63808

Suryani, Musnina W.O.S., Ruslin, Nisa M, Aprianti R, & Hasanah M. (2019). Formulation and physical characterization of curcumin nanoparticle transdermal patch. *International Journal of Applied Pharmaceutics*, 11(6), 217–221. http://dx.doi.org/10.22159/ijap.2019v11i6.34780

Syaefudin, Oktovianti, V., & Andrianto, D. (2023). Formulasi dan evaluasi krim antijerawat berbahan limbah cangkang kerang bulu (*Anadara antiquata* Linn.). *Jurnal Pengolahan Hasil Perikanan Indonesia*, 26(2), 314-325. https://doi.org/10.17844/jphpi.v26i2.44109

Usman, J.T., Aliyah, Nur, J.F., Nirmayanti, & Permana, A.D. (2023). Combinatorial approach of polymeric patches and solid microneedles for improved transdermal delivery of valsartan: a proof-of-concept study. *Biointerface Research in Applied Chemistry*, 13(4), 314. https://doi.org/10.33263/BRIAC134.314

Vaz, J.M.,Taketa,T.B., Hernandez-Montelongo,J., Chevallier, P., Cotta, M.A., Mantovani, D., & Beppu, M.M. 2018. Antibacterial properties of chitosan-based coatings are affected by spacer-length and molecular weight. *Applied Surface Science*, 445, 478-487. https://doi.org/10.1016/j.apsusc.2018.03.110

Vivcharenko, V., Benko, A., Palka, K., Wojcik, M., & Przekora, A. (2020). Elastic and biodegradable chitosan/agarose film revealing slightly acidic ph for potential applications in regenerative medicine as artificial skin graft. *International Journal of Biological Macromolecules*,164, 172–183. https://doi.org/10.1016/j.ijbiomac.2020.07.099

Wu, J., Wang, Y., Yang, H., Liu, X., & Lu, Z. (2017). Preparation and biological activity studies of resveratrol loaded ionically cross-linked chitosan-TPP nanoparticles. *Carbohydrate Polymers*, 175, 170–177. https://doi.org/10.1016/j.carbpol.2017.07.058

Zhang, Y., Feng, P., Yu, J., Yang, J., Zhao, J., Wang, J., Shen, Q. & Gu, Z. (2018). ROS-Re sponsive Microneedle Patch for Acne Vulgaris Treatment. *Advanced Therapeutic*, 1(3), 1800035. https://doi.org/10.1002/adtp.201800035

Zhang, T., Sun, B., Guo, J., Wang, M., Cui, H., Mao, H., Wang, B., & Yan, F. (2020). Active pharmaceutical ingredient poly(ionic liquid)-based microneedles for the treatment of skin acne infection. *Acta Biomater*, 115, 136-47. https://doi.org/10.1016/j.actbio.2020.08.023

Zmejkoski, D. Z., Markoviæ, Z. M., Budimir, M. D., Zdravkoviæ, N. M., Trišiæ, D. D., Bugárová, N., Danko, M., Kozyrovska, N. O., Špitalský, Z., Kleinová, A., Kuzman, S. B., Pavloviæ, V. B., & Todoroviæ Markoviæ, B. M. (2021). Photoactive and antioxidant nanochitosan dots/biocellulose hydrogels for wound healing treatment. *Materials Science and Engineering, 122*(1). https://doi.org/10.1016/j.msec.2021.111925